Development of Fuel Debris Inspection Methods using Air-Coupled Ultrasound

Ari Hamdani[1+], *Hiroshige* Kikura[1], *Shun* Kimura[1], *Keisuke* Tsukada[1], *Daisuku* Sasa[2], and *Shuichi Oomori*[2]

[1]Laboratory for Advanced Nuclear Energy Tokyo Institute of Technology Tokyo, Japan
[2]Tokyo Electric Power Company Holding (TEPCO) Yokohama, Japan

Abstract. Japan has decided to start fuel debris removal on 2021. Therefore, before starting retrieval of the fuel debris, investigation of location, shape, and also properties of fuel debris have to be performed. In this study, air-coupled ultrasound technique had been developed in order to visualize of fuel debris. Firstly, simulated fuel debris was represented by stone and experiment was done in laboratory scale. Flat and focused air-coupled ultrasound were used as a sensor to get echo signals of the target surface. Results showed that both flat and focused sensor successfully reconstructed the flat surface image in good spatial resolution. However, flat air-coupled transducer shown unstructured. On the other hand, focused air-coupled ultrasound shown good performance when target surface was unstructured. Therefore, it was recommended to used focused sensor when target surface was unstructured like simulated fuel debris.

1. Introduction

On March 11, 2011, a massive earthquake and tsunami struck Tohoku area of Japan. As a consequence, there was a severe accident on Fukushima Daiichi Nuclear Power Plant (NPP). This accident released a significant quantity of radionuclides into the environment and three of the plant's six reactors suffered core meltdowns (unit 1,2 and 3). A report by Tokyo Electric Power Company (TEPCO) [1], in unit 1 almost all of melted fuel has fallen down to the Primary Containment Vessel (PCV) and little fuel has left in Reactor Pressure Vessel (RPV). For unit 2 and 3, some part of melted fuels has fallen down to the bottom of RPV plenum and PCV pedestal and the other part may have fallen left inside RPV. Recently, fuel removal completed in unit 4 on December 22, 2014. Hence, retrieval of the debris, especially in unit 1, 2 and 3, is the primary requirement for the ending, of the accident. However, the way toward retrieval of debris is long tough, In mid-and-long-term decommissioning roadmap by TEPCO, fuel debris retrieval is expected to begin on 2021 [2].

Therefore, efficient and reliable technology for removal fuel debris is indispensable. First of all, the location, the shape, and also the properties of debris have to be investigated, while it is continuing refusing human's approach by generating extremely high-level radiation. Currently, researchers have identified two methods for retrieving highly radioactive nuclear fuel debris in three reactors at Tokyo Electric Power Company's (Tepco's) Fukushima Daiichi plant [3]. They are submersion method and dry method as shown in Figure 1. Before perfoming a retrieval fuel debris, the shape of fuel debris in RPV and PCV must be visualized. A nondestructive inspection method for identifying the position and shape of fuel debris is indispensable. The novel measurement technique for fuel debris visualization mush have these features [3]:

1. Enable remote control to keep low exposures for workers.
2. Avoid interference with existing structures.
3. Adapt to operations in air (high dose and high humidity).
4. Enable long continuous use.

A previous study, Takegami et al. [4] investigated internal visualization of the High-Temperature Engineering Test Reactor (HTTR) of Japan Atomic Energy Agency by using cosmic-ray muons. Such as concrete walls of the containment vessel of the HTTR. From the results of the preliminary examination, it appears that the inspection method with muons is promising for searching for fuel debris in a reactor. However, another measurement technique must be developed when muon technique cannot be used in good order. As shown in Figure 1.b., the novel measurement technique must adapt to operations in the air with high dose radiation and humidity.

When the dry method is used a retrieving fuel debris, ultrasound technique can be a good candidate for visualization mehtod. Generally, ultrasound technique needs a coupling medium such as water for better ultrasound's signal propagation. Nevertheless, ultrasound imaging in the air is advatageous because the position of the transducers can be set freely. Furthermore, imaging in the air provides higher resolution than in water because the sound wavelength is shorter in air at a given frequency [5]. Fox *et al*. [6] successfully demonstrated ultrasonic images visualization by 2 MHz using an air-coupled transducer. Consequently, based on previous studies, a measurement technique for fuel debris inspection is developed in our laboratory. The objective of this study is to visualize the shape of fuel debris surface in laboratory scale. A preliminary experiment is conducted at room temperature and a stone represents as simulated fuel debris.

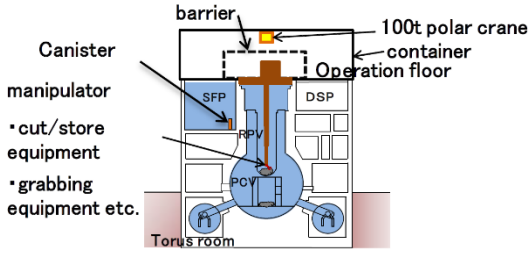

Fuel debris cut and stored under water

a. Submersion method

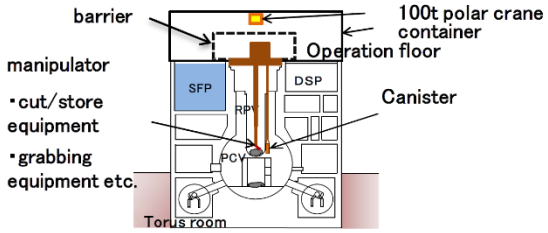

Fuel debris cut and stored in air

b. Dry method

Fig. 1. Fuel debris retrieval methods [3].

2. Experimental Apparatus

2.1 Air-coupled ultrasound transducer

Generally, ultrasound technique needs a coupling medium such as water for better ultrasound's signal propagation. Air-coupled ultrasound is a non-contact method, thus the difference of acoustic impedance must be taken care. The transmission of two media with high difference acoustic impedance e.g. piezo-electric ceramic (Z_{pc}) and air (Z_a) can be reduced by using a matching layer. Therefore, the ultrasonic wave passes with three different acoustic impedances as shown in Fig.2.

The total energy transmission coefficient is given by

$$T_{I_{total}} = \frac{4.Z_{pc}.Z_a}{\left(\frac{Z_a}{Z_{pc}}+1\right)^2 - \left(\left(\frac{Z_a}{Z_{ml}}\right)^2 - 1\right).\left(\left(\frac{Z_{ml}}{Z_{pc}}\right)^2 - 1\right).\sin^2 kd} \quad (1)$$

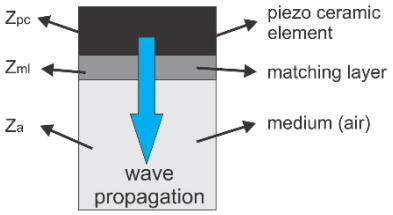

Fig. 2. Impedance matching layer between piezo-electric ceramic and air.

Where Z_{pc}, Z_a and Z_{ml} are the acoustic impedance of piezoelectric ceramic, air and matching layer. K is a wave number of the matching layer and d is matching layer thickness. In this study, flat (0.4K×20N-RX) and focused (0.4K20N) air-coupled ultrasound transducers are used as shown in Fig.3. These two transducers are manufactured by Japan Probe and the basic frequency is 400kHz.

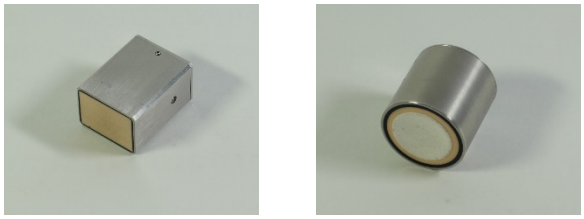

a. flat (0.4K×20N-RX) - sensor A b. focused (0.4K20N) - sensor B

Fig. 3. air-coupled ultrasound transducers.

2.2 Experimental procedure

The basic theory of air-coupled ultrasonic visualization method is simple because it depends mainly on the sound velocity through the air. The air-coupled transducers scans across the surface and sends ultrasound waves to the sample surface, the ultrasound waves are reflected back from the surface along the same path as the incident ultrasound wave. Time-of-flight images of the sample surface are acquired and converted to depth / surface profile images using the simple relation

$$d = \frac{c.t}{2} \quad (2)$$

Where d is distance, t is time-of-flight and c are the velocities of sound in air. In this experiment, three-dimension stage automation is used to move air-coupled ultrasound transducer and visualize the three-dimensional shape of the target. The experiment apparatus is constructed and the simplification experimental apparatus is shown in Figh.4.

Transmission and reception of ultrasonic wave are perfomed by using Japan Probe Co. Pulse-receiver (JPR-10CN). Three-axis stage automation is made by Sigma Koki (OSM26-300 (X) and OSM26-200 (Z)) and controlled by stage controller (SHOT-304GS). Both pulse receiver and three-dimension stage automation are controlled by self-made software as shown in Fig.5.

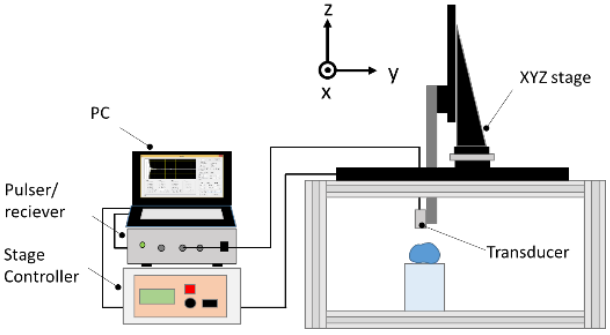

Fig. 4. Air-coupled ultrasound experimental apparatus.

Firstly, pulse-receiver sends an electrical signal to the sensor, then the ultrasonic wave is propagated in the air and reflected back to the sensor by the reflector. The received signal is then converted to a digital signal using AD converter and recorded by the personal computer. The control program has functional as below:

1. Direct control of pulse-receiver e.g. frequency, excitation voltage, wave number, high pass filter, low pass filter, etc.
2. Send and receive an ultrasonic wave and display the received signal.
3. Directly control the stage automation in the x, y, z-direction.
4. Display and storage the echo signals while scanning in the x,y, z-direction.

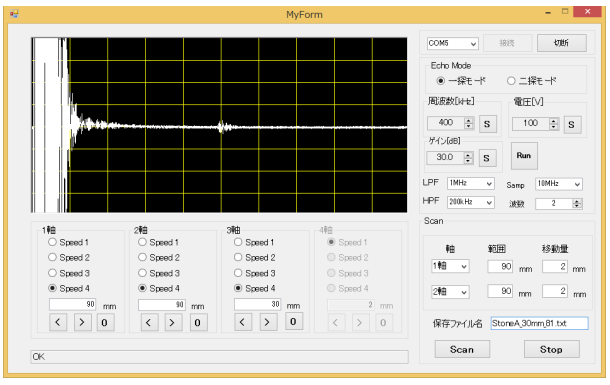

Fig. 5. Device's control program.

Figure 6 and 7 shows the reference reflector and simulated debris are used in this experiment.. A cylindrical stainless steel with 50 mm diameter and 50 mm in height is used as a reference reflector. Simulated fuel debris is represented by a stone with unstructured shape's surface.

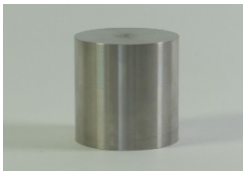

Fig. 6. Cylindrical stainless steel's reflector (reference reflector).

Fig. 7. Simulated fuel debri's reflector.

The preliminary test of the echo signal measurement is done for both reflectors. In the experiment, the ultrasound transduceer z-axis is moved to the positive direction, to observe the change of the echo signal while changing the distance between the reflector and an ultrasonic transducer. The positional relationship between the sensor and the reflector is shown in Fig.8. The reflector is placed on top of the acrylic block 90 × 90 × 90 mm, the initial distance (*H*) to the center of the reflector is set 10 mm. The air-coupled transducer transmits ultrasonic waves from 10 mm to the target surface, then continued to another position by every 5 mm in the *z* direction. Measurement settings for air-coupled ultrasound are shown in Table 1.

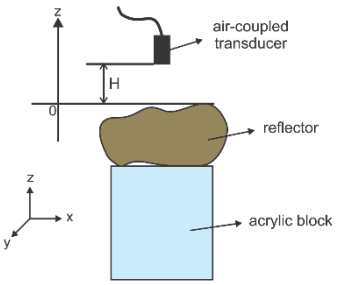

Fig. 8. The position between the sensor and reflector.

Table 1. Measurement Settings

Parameter	Value
Voltage	100 V
Basic frequency	400 kHz
Wave number	2
Gain	30 dB
Low pass filter	1 MHz
High pass filter	200 kHz
Sampling rate	10 MHz

The reconstruction of the two-dimensional image is performed for both reference reflector and simulated fuel debris. Flat transducer sensor (sensor A) and focused sensor (sensor B) are used to acquire echo signals in every 2 mm either x or y-direction. Measurement of the echo signals is automatically controlled by three-dimensional stage automation and the distance of sensor to the reflector's center is determined by echo signals measurement results. Reconstruction image is constructed by seeking time of flight at every measurement position point. Therefore, the distance between sensor and target surface can be obtained by Eq. 1.

3. RESULTS AND DISCUSSIONS

3.1 Echo signals (preliminary experiment)

Figure 9 shows an example of the echo signals coming from the surface of the reference reflector measured by sensor A. It can be seen that echo signals from the cylinder surface can be obtained. Furthermore, it can be confirmed that time of flight and echo signal's intensity change when the distance H is changed in the z direction. The time of flight represents a distance between sensor and target surface. However, at H = 10 and H = 15 mm, the echo signals from target surface are difficult to be distinguished. It is due to near field or dead zone region (below 200 μs) close to transducer's surface. Thus, it is recommended to set initial distance (H) at least 30 mm from the target surface.

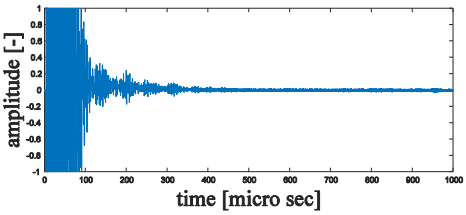

a. H = 10 mm

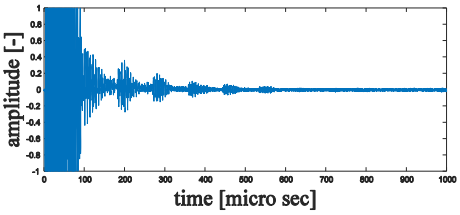

b. H = 15 mm

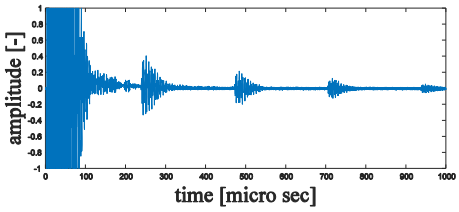

c. H = 40 mm

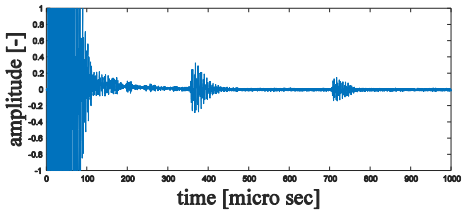

d. H = 60 mm

Fig. 9. Echo signal of the reference reflector measured by sensor B.

Figure 10 shows echo signals coming from reference reflector measured by sensor B. It can be seen that focused air-coupled ultrasound sensor sufficiently obtain echo signals from the target surface. Furthermore, comparing to the results in Figure 9, the echo signal's intensity measured by sensor B is higher. It means that sensor B has better sensitivity compare with sensor A. However, it can be found that dead zone still appears below 100 μs.

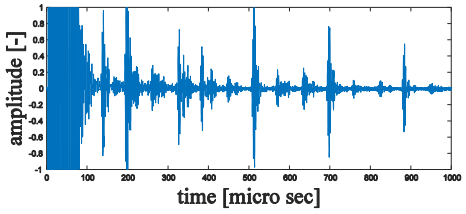

a. H = 10 mm

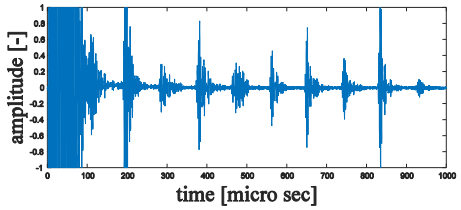

b. H = 15 mm

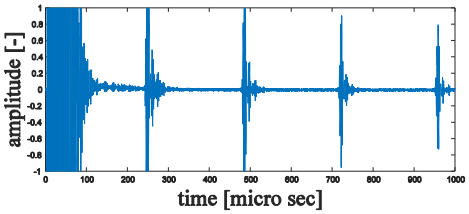

c. H = 40 mm

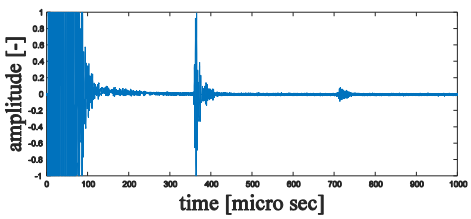

d. H = 60 mm

Fig. 10. Echo signal of the reference reflector measured by sensor B.

Figure 11 and 12 show echo signals coming from simulated fuel debris reflector measured by sensor A and B respectively. It can be seen in Fig. 11 that echo signals cannot be obtained in any distance H, it is due to the irregularity of target surface. As a result, neither reflected ultrasound wave is not received by sensor nor attenuated. On the other hand, measured echo signals are possible using sensor B as shown in Fig. 12. Because of sensor B has a curvature on its surface, thus ultrasound wave can be focused into a small area of the target surface. In addition, echo signals which are obtained by sensor B are distinguishable. But still, dead zone (near field region) cannot be avoided.

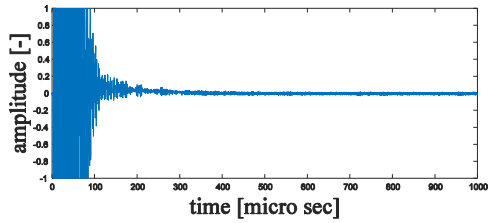

a. H = 10 mm

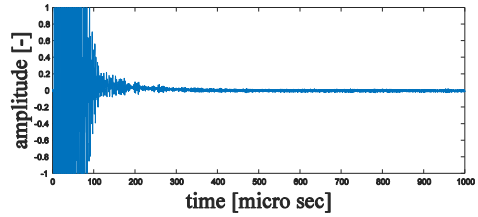

b. H = 15 mm

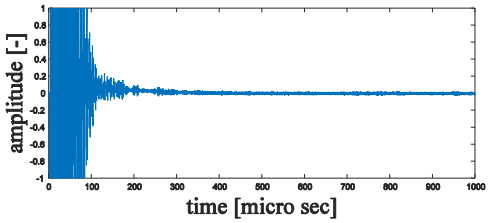

c. H = 40 mm

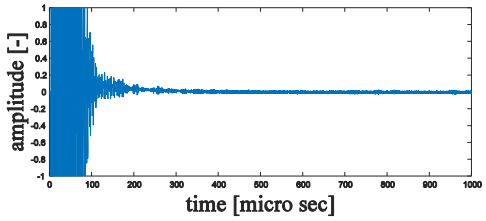

d. H = 60 mm

Fig. 11. Echo signal of the simulated fuel debris reflector measured by sensor A.

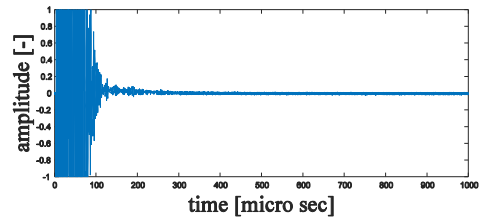

a. H = 10 mm

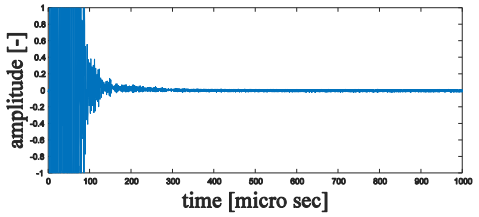

b. H = 15 mm

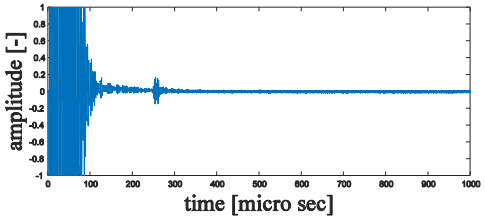

c. H = 40 mm

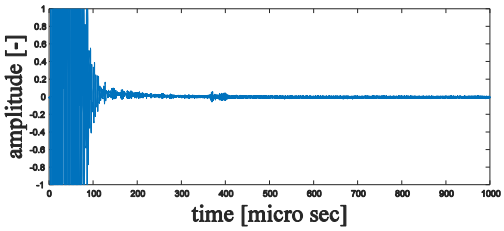

d. H = 60 mm

Fig. 12. Echo signal of the simulated fuel debris reflector measured B.

3.2 Image reconstruction

By using time of flight information, it is possible to reconstruct a three-dimensional image. Echo signals are being obtained while the sensor is scanning on the x-y plane. The distance between sensor and target (H) is set 30 mm. Then, shapes of both reference reflector and simulated fuel debris are constructed. The image reconstruction is developed using MATLAB®R2016a. Results are shown in Fig. 13 and 14. Figure 13 shows the image reconstruction of reference reflector by sensor A and Fig. 14 shows the image reconstruction of reference reflector by sensor B.

Figure 13a and 14a show the reconstruction image of reference reflector in the x-y plane, the horizontal axis is a distance in the x-direction and the vertical axis is a distance in the y-direction. Red color means that the distance between sensor and reflector is short (in this case is equal to 30 mm, H) and blue color means that the distance between sensor and reflector is far (in this case is equal to 80 mm). It can be confirmed that the radius of reference reflector is 50 mm. In addition, depth of reference reflector is known by subtracting the maximum depth (blue color) with the initial distance H. Thus, the height of reference reflector is confirmed 50 mm. Figure 13b and 14b show the bird's eye view of reference reflector using sensor A and B respectively. It can be seen that three-dimensional

shape is fully obtained. Furthermore, image reconstruction results measured by sensor A and B show similarity shape.

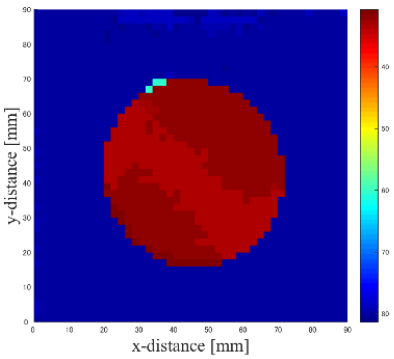

a. Image reconstruction in the x-y plane.

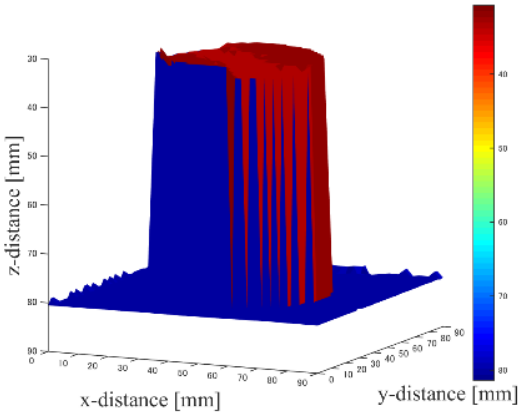

b. Image reconstruction in bird's eye view.

Fig. 13. Image reconstruction of reference reflector using sensor A.

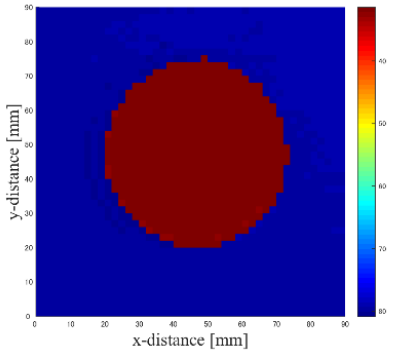

a. Image reconstruction in the x-y plane.

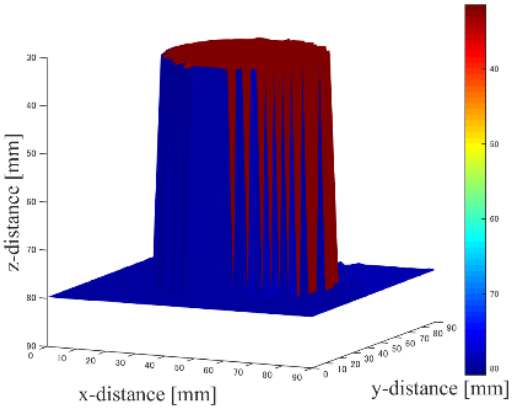

b. Image reconstruction in bird's eye view.

Fig. 14. Image reconstruction of reference reflector using sensor B.

Figure 15 shows the photograph of simulated fuel debris in the *x-y* plane (top view). This simulated fuel debris is scanned in *x-y* direction using both sensor A and B. Figure 16 shows reconstruction image of simulated fuel debris measured by sensor A in the *x-y* plane and Fig. 17 shows reconstruction image of simulated fuel debris measured by sensor B in the *x-y* plane. It can be seen that reconstruction image using sensor A is not clear compared with sensor B. It is because ultrasound's echo signals are greatly attenuated mainly due to scattering. As shown in preliminary experiment, it is difficult to get echo signals when sensor A is used in unstructured surfaced. Therefore, when sensor A is used, a distance between sensor and target surface can be calculated accurately. On the other hand, reconstruction image of fuel debris measured by sensor B has good accuracy. It can be seen in Fig. 17 that sensor B has a better result when target surface is unstructured.

Fig. 15. Simulated fuel debris in the x-y plane.

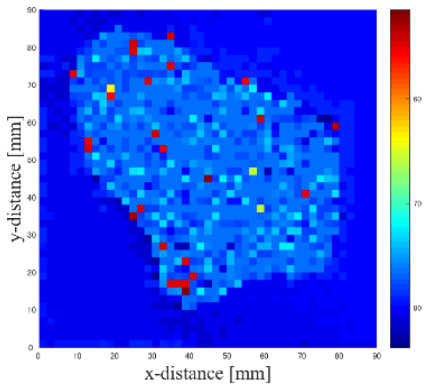

Fig. 16. Image reconstruction of simulated fuel debris sensor A in the x-y plane.

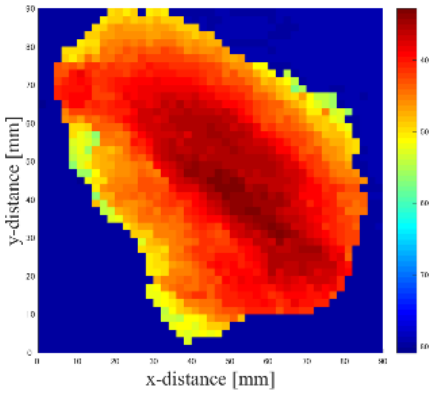

Fig. 17. Image reconstruction of simulated fuel debris using sensor B in the x-y plane.

4. Conclusion

Object visualization using air-coupled ultrasound is successfully developed. This measurement technique can be used as fuel debris inspection before removal the fuel debris is done. Hence, air-coupled measurement technique can be alternative technology in order to know the shape and size of fuel debris when the dry method is used. These are the following conclusions in this study.

1. The advantage of the air-coupled ultrasonic sensor was no need coupling fluid i.e. water. Thus, an acoustical mismatch between solids (transducers, test component) and air (coupling medium) must be taken care. This acoustical mismatch could be reduced by using matching layer.
2. Flat and focused air-coupled ultrasonic were good to get echo signals for flat target surface. However, the flat sensor had worse performance when the target surface was unstructured. It was due to ultrasound echo signals were greatly attenuated.
3. By using time-of-flight information, it was possible to reconstruct an image of the target surface. The spatial resolution of focus sensor shown good accuracy compared with the flat transducer. Therefore, it is recommended to used focused sensor when target surface is unstructured like simulated fuel debris.

References

1. A. Komori, *49th JAIF Annual Conference*, 1-33 (2016)
2. T. Shinkawa, Revised mid-and-long-term roadmap towards the decommisioning of TEPCO's Fukushima Daiichi NPP Units 1-4, Ministry of Economy, Trade and Industry (METI) workshop, pp. 1-23, (2013)
3. K. Takamori, *The 1st International Forum on the Decommissioning of the Fukushima Daiichi Nuclear Power Station*, 1-32 (2016)
4. H. Takegami, K. Takamatsu, C. Ito, R. Hino, K. Suzuki, H. Ohnuma, T. Okumura, Nippon Genshiryoku **13**, 7-16 (2014)
5. S. Takahashi, H. Ohigashi, Ultrasonics **49**, 495-498 (2009)
6. J.D. Fox, G.S. Kino, B.T. Khuri-Yakub, Appl. Phys. Lett. **47**, 465-467 (1985)